Long non-coding RNA *PEG13* regulates endothelial cell senescence through the microRNA-195/IRS1 axis

QIN HUANG[*], HAIWEN ZHOU[*] and SONGPING YU

Department of Cardiology, Jiangxi Provincial People's Hospital, The First
Affiliated Hospital of Nanchang Medical College, Nanchang, Jiangxi 330006, P.R. China

Abstract. Atherosclerosis is a chronic inflammatory disease characterized by endothelial dysfunction and plaque formation. The present study aimed to elucidate the pathological role of the long non-coding RNA (lncRNA) paternally expressed 13 (*PEG13*) in the onset and progression of atherosclerosis. Specifically, its effects on human umbilical vein endothelial cell (HUVEC) proliferation, angiogenesis, senescence and senescence-associated secretory phenotype (SASP)-related factors were investigated using cell proliferation, cellular angiogenesis, β-galactosidase staining, reverse transcription-quantitative PCR and enzyme-linked immunosorbent assays. The results showed that oxidized low-density lipoprotein (ox-LDL) inhibited lncRNA *PEG13* expression and HUVEC viability in a dose-dependent manner and *PEG13* overexpression partially reversed these effects. Additionally, *PEG13* overexpression ameliorated the ox-LDL-induced impairment of angiogenesis, cellular senescence and SASP. Furthermore, lncRNA *PEG13* directly targeted microRNA (miR/miRNA)-195-5p, suppressing the ox-LDL-induced upregulation of the miRNA. The gene coding for insulin receptor substrate 1 (*IRS1*), an activator of the phosphoinositide 3-kinase (PI3K)/protein kinase B (AKT) signaling pathway, was confirmed as a direct target of miR-195. *PEG13* overexpression attenuated the ox-LDL-induced inhibition of *IRS1* expression and PI3K/AKT signaling and its protective effects on HUVEC viability, angiogenesis and senescence were partially reversed by small interfering RNAs targeting *IRS1*. The present study demonstrated that lncRNA *PEG13* attenuates ox-LDL-induced senescence in HUVECs by modulating the miR-195/IRS1/PI3K/AKT signaling pathway, suggesting a potential therapeutic target for the treatment of atherosclerosis.

Correspondence to: Dr Songping Yu, Department of Cardiology, Jiangxi Provincial People's Hospital, The First Affiliated Hospital of Nanchang Medical College, 152 Aiguo Road, Nanchang, Jiangxi 330006, P.R. China
E-mail: ysp18942337985@126.com

Abbreviations: RT-qPCR, reverse transcription-quantitative PCR; WT, wild type; mut, mutant; miRNA/miR, microRNA; NC, negative control; ox-LDL, oxidized low-density lipoprotein; lncRNA, long non-coding RNA; *PEG13*, paternally expressed gene 13; SASP, senescence-associated secretory phenotype; MDM2, MDM2 proto-oncogene; MCP-1, monocyte chemoattractant protein-1; VCAM-1, vascular cell adhesion molecule-1; ICAM-1, intercellular adhesion molecule-1; GAPDH, glyceraldehyde 3-phosphate dehydrogenase; HUVECs, human umbilical vein endothelial cells; IRS1, insulin receptor substrate 1; p, phosphorylated; siRNA, small interfering RNA; MTT, 3-(4,5-dimethylthiazol-2-yl)-2,5-diphenyltetrazolium bromide; SA-β-gal, senescence-associated beta-galactosidase; ELISA, enzyme-linked immunosorbent assay; p53, tumor protein p53; p21/CDKN1A, cyclin-dependent kinase inhibitor 1A

[*]Contributed equally

Introduction

Atherosclerosis, a chronic progressive inflammatory disease, is a major cause of morbidity and mortality associated with cardiovascular diseases worldwide (1). The hallmark of atherosclerosis is the accumulation of oxidized low-density lipoprotein (ox-LDL) in the arterial wall, which leads to endothelial dysfunction, chronic inflammation and ultimately plaque formation (2). However, the pathological mechanisms underlying this vascular disease remain to be elucidated.

Endothelial cell senescence is a major driver of atherosclerosis and induces the secretion of pro-inflammatory cytokines and chemokines (3), a phenomenon termed the senescence-associated secretory phenotype (SASP) (4). Among the SASP components, IL-1β, IL-6 and IL-8 are key factors in the local inflammatory milieu of the arterial wall, whereas monocyte chemoattractant protein-1 (MCP-1), vascular cell adhesion molecule-1 (VCAM-1) and intercellular adhesion molecule-1 (ICAM-1) coordinate the recruitment and adhesion of monocytes and immune cells (5,6). These mediators drive the inflammatory cascade, leukocyte recruitment and adhesion in atherosclerosis, making their targeted inhibition critical for the treatment of this vascular condition.

In recent years, non-coding RNAs such as microRNAs (miRNAs/miRs) and long non-coding RNA (lncRNAs) have been found to play critical roles in regulating the functions of endothelial cells and the pathogenesis of atherosclerosis. In particular, miR-195-5p (miR-195) acts as an inflammatory

inducer in various cell types, such as vascular smooth muscle cells (7) and chondrocytes (8), and its overexpression impairs the angiogenesis of human umbilical vein endothelial cells (HUVECs) (9). The inhibition of miR-195 expression has been shown to attenuate atherosclerosis (10). Additionally, the novel lncRNA paternally expressed gene 13 (*PEG13*) has been shown to function as a competitive endogenous RNA to attenuate neuroinflammation (11) and reduce apoptosis (12). However, the role and mechanism of action of lncRNA *PEG13* in atherosclerosis remain to be elucidated.

PI3K/AKT signaling is a key regulator of various cellular processes, including proliferation, inflammation and senescence and has emerged as an important participant in the modulation of endothelial cell function and atherosclerosis progression (13-15). Activation of the PI3K pathway leads to the activation of AKT, which directly phosphorylates the MDM2 proto-oncogene (MDM2) at residues Ser166 and Ser186 (16). MDM2 activation promotes endothelial cell survival and attenuates senescence (17), in part by inhibiting tumor protein p53 (p53) and its downstream effector, cyclin-dependent kinase inhibitor 1A (CDKN1A; p21) (18). Additionally, insulin receptor substrate 1 (IRS1) signaling has been identified as an upstream effector of the PI3K/AKT pathway, contributing to the regulation of cellular senescence and inflammation (19,20). Notably, Wang *et al* (21) showed that *IRS1* is a target gene of miR-195.

The present study aimed to elucidate the potential roles of lncRNA *PEG13*, miR-195, IRS1 and the PI3K/AKT signaling pathway in regulating endothelial cell senescence, SASP and atherosclerosis development. By elucidating the underlying molecular mechanisms, it was hoped to deepen our understanding of the pathophysiology of atherosclerosis and reveal novel therapeutic targets for the development of new strategies for its treatment.

Materials and methods

Screening of mRNA and signaling pathways. The GSE109048 dataset (22) (http://www.ncbi.nlm.nih.gov/geo/) was analyzed using the dataset analysis tool GEO2R (version R 3.2.3; https://www.ncbi.nlm.nih.gov/geo/geo2r/) and the differential expression of mRNAs between tissue samples from healthy donors and those from patients with atherosclerosis was normalized to log2|fold change|>1, with P<0.05. The Kyoto Encyclopedia of Genes and Genomes (KEGG) database (https://www.kegg.jp/) was used for pathway enrichment analysis of the mRNAs to identify the major pathways involved in atherosclerosis progression.

Cell culture and transfection. Human umbilical vein endothelial cells (HUVECs) were obtained from the American Type Culture Collection and cultured in endothelial cell culture medium (cat. no. CM-0122; Procell Life Science & Technology Co., Ltd.). Prior to transfection, the HUVECs were seeded at a density of $2x10^5$ cells/well in a 6-well plate and were exposed to different doses (0, 25, 50, 100 and 200 μg/ml) of ox-LDL (Beijing Solarbio Science & Technology Co., Ltd.) for 24 h. Following transfection, the cells were divided treated with 100 μg/ml of ox-LDL for 24 h to simulate the atherosclerotic environment *in vitro*. To investigate the role of the PI3K/AKT

pathway in ox-LDL-induced HUVEC senescence, these atherosclerotic cells were also incubated with either 10 μM LY294002 (Beijing Solarbio Science & Technology Co., Ltd.) for 30 min to inhibit PI3K signaling or dimethyl sulfoxide (DMSO; Beijing Solarbio Science & Technology Co., Ltd.) as the control group. The lncRNA *PEG13* overexpression (ov) vector, overexpression negative control (NC) and miR-195 mimic/inhibitor were purchased from GenePharma (Shanghai, China), and the sequences of the RNAs are listed in Table SI. RNA transfections were performed using Lipofectamine® 3000 according to the manufacturer's instructions (Invitrogen; Thermo Fisher Scientific, Inc.) at 37°C for 4 h. *PEG13* overexpression vector and ov-NC were used at a mass of 2 μg/well and miR-195 mimic/inhibitor was used at a dose of 50 nM. At 24 or 48 h post-transfection, cells were collected for gene detection or protein level detection.

Nucleocytoplasmic separation and reverse transcription-quantitative (RT-q)PCR. To investigate the subcellular localization of lncRNA *PEG13*, a nucleocytoplasmic separation assay was performed using the NE-PER Nuclear and Cytoplasmic Extraction Kit (Thermo Fisher Scientific, Inc.) according to the manufacturer's instructions. The cytoplasmic and nuclear fractions were both used for subsequent RNA isolation and RT-qPCR analysis to determine their relative expression levels of lncRNA *PEG13*. Total RNA was isolated from HUVECs ($4x10^5$ cells) using TRIzol® reagent (Thermo Fisher Scientific, Inc.) according to the manufacturer's instructions and RNase-free DNase I (Promega Corporation) was used to digest the genome. The RNA concentration was determined using a BioPhotometer Plus spectrophotometer (Eppendorf Ltd.), following which the RNA was reverse transcribed to complementary DNA (cDNA) using a cDNA synthesis kit (Invitrogen; Thermo Fisher Scientific, Inc.) according to the manufacturer's protocol. The RT-qPCR was performed using the One-Step SYBR Green RT-qPCR Kit (Biomarker Technologies, Inc.) according to the manufacturer's protocol. Primers specific for the target genes (lncRNA *PEG13*, miR-195 and *IRS1*) and a reference gene (β-actin or *U6*) were used (sequences listed in Table SII). The PCR cycling conditions were as follows: an initial denaturation step at 95°C for 1 min, followed by 40 cycles of denaturation at 95°C for 12 sec, annealing at 60°C for 32 sec and extension at 72°C for 30 sec. The relative expression levels of the target genes were calculated using the $2^{-\Delta\Delta Cq}$ method (23).

RNA pull-down assay. Biotin-labeled lncRNA *PEG13*, miR-195 and their mutant (mut) probes were synthesized and purified by means of *in vitro* transcription using the Biotin RNA Labeling Mix (GenePharma) and lysed using RIPA buffer (Beijing Solarbio Science & Technology Co., Ltd.) according to the manufacturer's instructions. After pre-clearing with streptavidin magnetic beads (Thermo Fisher Scientific, Inc.), the cell lysate was incubated overnight with the biotin-labeled lncRNA *PEG13*, miR-195, or mut probes at 4°C. Streptavidin magnetic beads were then added and the mixture was incubated for 2 h at 4°C. Subsequently, the beads were thoroughly washed and the bound RNA was eluted and extracted using TRIzol® reagent. The presence of miR-195 or lncRNA *PEG13*

in the eluted RNA solution was analyzed using RT-qPCR as aforementioned.

Western blotting. After the HUVECs had been lysed with lysis buffer (Beijing Solarbio Science & Technology Co., Ltd.), the protein levels were determined using a bicinchoninic acid protein assay kit (Beijing Solarbio Science & Technology Co., Ltd.) according to the manufacturer's instructions. The denatured proteins (20 μg) were separated using sodium dodecyl sulfate-polyacrylamide gel electrophoresis (10%) and transferred to polyvinylidene fluoride membranes (MilliporeSigma). Then, the membranes were rinsed with 10% Tween 20-containing Tris-buffered saline (TBST; Beijing Solarbio Science & Technology Co., Ltd.), blocked with 5% bovine serum albumin (Beijing Solarbio Science & Technology Co., Ltd.) at 22˚C for 1 h, and incubated overnight with primary antibodies against IRS1 (1:1,000; cat. no. MA5-15068; Invitrogen; Thermo Fisher Scientific, Inc.), PI3K (1:1,000; cat. no. ab191606; Abcam), phosphorylated (p)-PI3K (1:500; cat. no. ab182651; Abcam), AKT (1:500; cat. no. ab8805, Abcam), p-AKT (1:500; cat. no. ab38449; Abcam), MDM2 (1:1,000; cat. no. ab259265; Abcam), p53 (1:2,000; cat. no. ab32049; Abcam), p21 (1:3,000; cat. no. ab109520; Abcam) and glyceraldehyde 3-phosphate dehydrogenase (GAPDH; 1:3,000; cat. no. ab181602; Abcam) at 4˚C. The membranes were then incubated with horseradish peroxidase-conjugated IgG H&L secondary antibodies (1:2,000; cat. no. ab205718; Abcam) for 2 h at 22˚C. Bands were visualized using Enhanced Chemiluminescence reagent (Thermo Fisher Scientific, Inc.). Densitometry analysis was performed using ImageJ software (version 1.8.0; National Institutes of Health).

Enzyme-linked immunosorbent assay (ELISA). The levels of IL-1β (cat. no. SEKH-0002), IL-6 (cat. no. SEKH-0013) and IL-8 (cat. no. SEKH-0016) in the culture supernatants of HUVECs were measured using ELISA kits (Beijing Solarbio Science & Technology Co., Ltd.) according to the manufacturer's instructions. In brief, cell debris was first removed from the collected culture supernatants through centrifugation at 1,000 x g for 5 min at 4˚C. ELISA plates were coated with capture antibodies specific for IL-1β, IL-6, or IL-8 and the samples were then added together with the corresponding standards. The absorbance was measured at 450 nm using a microplate reader (BioTek Instruments, Inc.).

Cell proliferation assay. HUVEC proliferation was assessed using the 3-(4,5-dimethylthiazol-2-yl)-2,5-diphenyltetrazolium bromide (MTT) assay. Cells (4.5×10^3/well) were seeded in 96-well plates and treated with ox-LDL for 24 h as previously indicated. After treatment, 20 μl of MTT solution (5 mg/ml) was added to each well and the plates were incubated at 37˚C for another 4 h. The medium was then gently aspirated and 150 μl of DMSO was added to dissolve the formazan crystals. The absorbance was measured at 570 nm using a microplate reader.

Cellular angiogenesis assay. Matrigel (BD Biosciences) was dissolved overnight at 4˚C and then diluted with precooled serum-free medium at a volume ratio of 1:3. Subsequently, 40 μl of the diluted solution was added to each well of a precooled 96-well plate, which was then incubated for 2 h at 37˚C to allow the Matrigel to coagulate. Thereafter, the Matrigel was covered with a 50 μl suspension of HUVECs (2×10^5 cells/per well) and the number of cell lumens was determined using an inverted microscope (Olympus Corporation).

Cellular senescence assay. Cellular senescence was assessed using a senescence-associated beta-galactosidase (SA-β-gal) staining kit (Cell Signaling Technology, Inc.) according to the manufacturer's instructions. In brief, HUVECs were washed with phosphate-buffered saline (PBS), fixed with 4% paraformaldehyde for 15 min at 22˚C and then incubated overnight with the manufacturer-provided SA-β-gal staining solution in a non-CO_2 incubator at 37˚C. The following day, the cells were washed with PBS and observed under a light microscope (Olympus Corporation). Senescent cells were identified by the blue staining of their cytoplasm.

Dual-luciferase reporter assay. The LncBase v3 (https://diana.e-ce.uth.gr/lncbasev3/interactions) and TargetScan 7.2 (https://www.targetscan.org/vert_72/) databases were used to predict the binding sites of miRNAs, lncRNAs and mRNAs. For the dual-luciferase reporter assay, either lncRNA *PEG13* (WT and mut) or IRS1 (WT and mut) sequence containing miR-195 binding sites were cloned into a pmirGLO luciferase reporter vector (Promega Corporation). Then, HUVECs were co-transfected with the luciferase reporter vector (WT or mut) and the miR-195 mimic or mimic NC at 37˚C for 4 h using Lipofectamine® 3000. After 48 h, the cells were lysed and their luciferase activity was measured using a dual-luciferase reporter assay system (Promega Corporation) according to the manufacturer's instructions. The firefly luciferase activity in each group was normalized to the *Renilla* luciferase activity to account for differences in transfection efficiency.

Statistical analysis. Data are expressed as the mean ± standard deviation and were analyzed using GraphPad Prism 8 (GraphPad Software; Dotmatics). The unpaired Student's t-test was used for comparisons between two groups. One-way or two-way analysis of variance was used to compare multiple groups, followed by Tukey's post-hoc test for pairwise comparisons. $P < 0.05$ was considered to indicate a statistically significant difference.

Results

Ox-LDL dose-dependently inhibited lncRNA PEG13 expression. In the present study, ox-LDL inhibited the viability of HUVECs (Fig. 1A) and the expression of lncRNA *PEG13* (Fig. 1B) in a dose-dependent manner. The ox-LDL dose of 100 μg/ml was selected for the subsequent mechanistic analyses. RT-qPCR verified the validity of the *PEG13* overexpression vector (Fig. 1C). Subsequently, it was observed that the reduced cell viability (Fig. 1D) and downregulation of *PEG13* expression (Fig. 1E) due to ox-LDL induction was reversed by *PEG13* overexpression. Moreover, *PEG13* overexpression alleviated the decline in angiogenic capacity (Fig. 1F) and the aggravated senescence (Fig. 1G) mediated by ox-LDL. Moreover, the ox-LDL-induced decrease in levels of
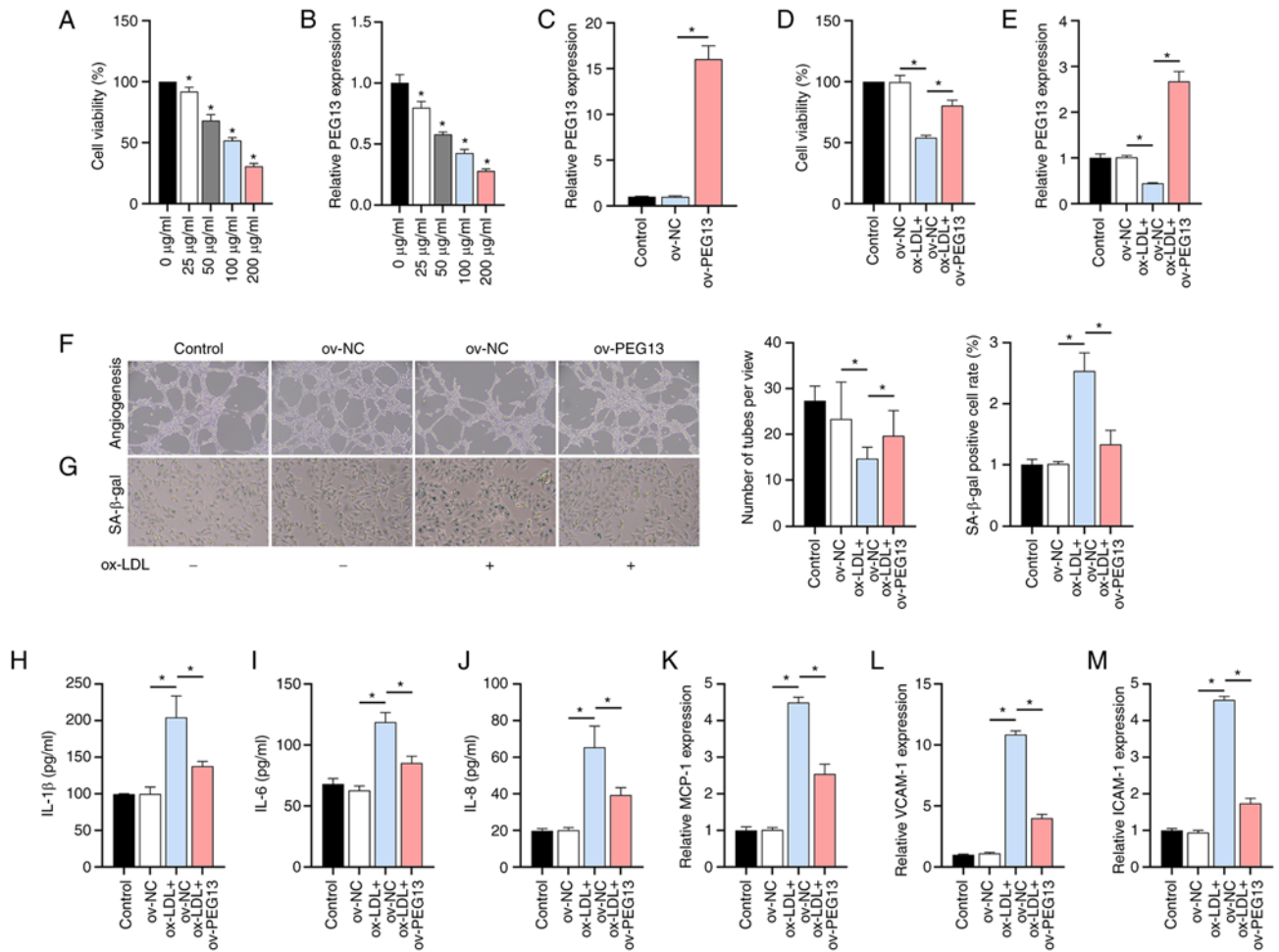
Figure 1. Effects of ox-LDL and lncRNA *PEG13* on HUVECs. (A) Dose-dependent inhibition of cell viability by ox-LDL, as determined with the MTT assay (*P<0.05 vs. 0 μg/ml). (B) LncRNA *PEG13* expression in response to ox-LDL, as determined through RT-qPCR analysis (*P<0.05 vs. 0 μg/ml). (C) Validation of the efficacy of the *PEG13* overexpression plasmid. (D) Effect of *PEG13* overexpression on cell viability under ox-LDL treatment, as determined with MTT assay. (E) *PEG13* expression in *PEG13*-overexpressing cells, as determined through RT-qPCR analysis. (F) Changes in angiogenic capacity due to *PEG13* overexpression, as determined by tube formation assay. Magnification, x200. (G) SA-β-gal staining showing the effect of *PEG13* overexpression on ox-LDL-induced senescence. Magnification, x200. (H-J) Levels of SASP-related factors (H) IL-1β, (I) IL-6 and (J) IL-8 following *PEG13* overexpression, as measured by ELISA. (K) MCP-1, (L) VCAM-1 and (M) ICAM-1 expression levels following *PEG13* overexpression, as determined through RT-qPCR analysis. *P<0.05. ox-LDL, oxidized low-density lipoprotein; lncRNA, long non-coding RNA; HUVECs, human umbilical vein endothelial cells; MTT, 3-(4,5-dimethylthiazol-2-yl)-2,5-diphenyltetrazolium bromide; RT-qPCR, reverse transcription-quantitative PCR; SASP, senescence-associated secretory phenotype; MCP-1, monocyte chemoattractant protein-1; VCAM-1, vascular cell adhesion molecule-1; ICAM-1 and intercellular adhesion molecule-1; ov, overexpression; SA-β-gal, senescence-associated beta-galactosidase; NC, negative control.

the SASP-related factors IL-1β, IL-6 and IL-8 was markedly enhanced by *PEG13* overexpression (Fig. 1H-J). Additionally, overexpression of this lncRNA enhanced the ox-LDL-induced inhibition of expression of the chemotactic/adhesive molecules MCP-1, VCAM-1 and ICAM-1 (Fig. 1K-M).

miR-195 identified as a potential target of PEG13. The high-level expression of cytoplasmic lncRNA *PEG13* was aligned with that of the positive control *GAPDH* and contrasted with the level of *U6* expression (Fig. 2A). Through LncBase database analysis, miR-195 emerged as a potential target of *PEG13* owing to its established association with adverse atherosclerosis prognosis (24). The RT-qPCR results showed that ox-LDL increased the miR-195 expression level in a dose-dependent manner (Fig. 2B), but this effect was suppressed by *PEG13* overexpression (Fig. 2C). After RT-qPCR confirmation of the efficacy of the synthesized miR-195 mimic/inhibitor (Fig. 2D), dual-luciferase reporter

assays were performed. Bioinformatics analysis revealed potential binding sites between lncRNA *PEG13* and miR-195 (Fig. 2E) and the dual-luciferase reporter assay confirmed reduced luciferase activity in the cells co-transfected with *PEG13*-WT and the miR-195 mimic. No significant difference was observed in the interaction between *PEG13*-mut and the miR-195 mimic or miR-NC (Fig. 2F). In the RNA pull-down assays, miR-195 and *PEG13* were enriched in the Bio-*PEG13* and Bio-miR-195 groups, respectively, whereas no significant changes were observed in the Bio-mut or Bio-miR-195-mut groups, which further confirmed their binding interaction (Fig. 2G and H). Additionally, the miR-195 mimic/inhibitor had no significant effect on *PEG13* expression (Fig. 2I). These results confirmed the direct targeting of miR-195 by lncRNA *PEG13*.

IRS1 is involved in the lncRNA PEG13/miR-195 axis. The joint analysis of the TargetScan and GSE109048 datasets
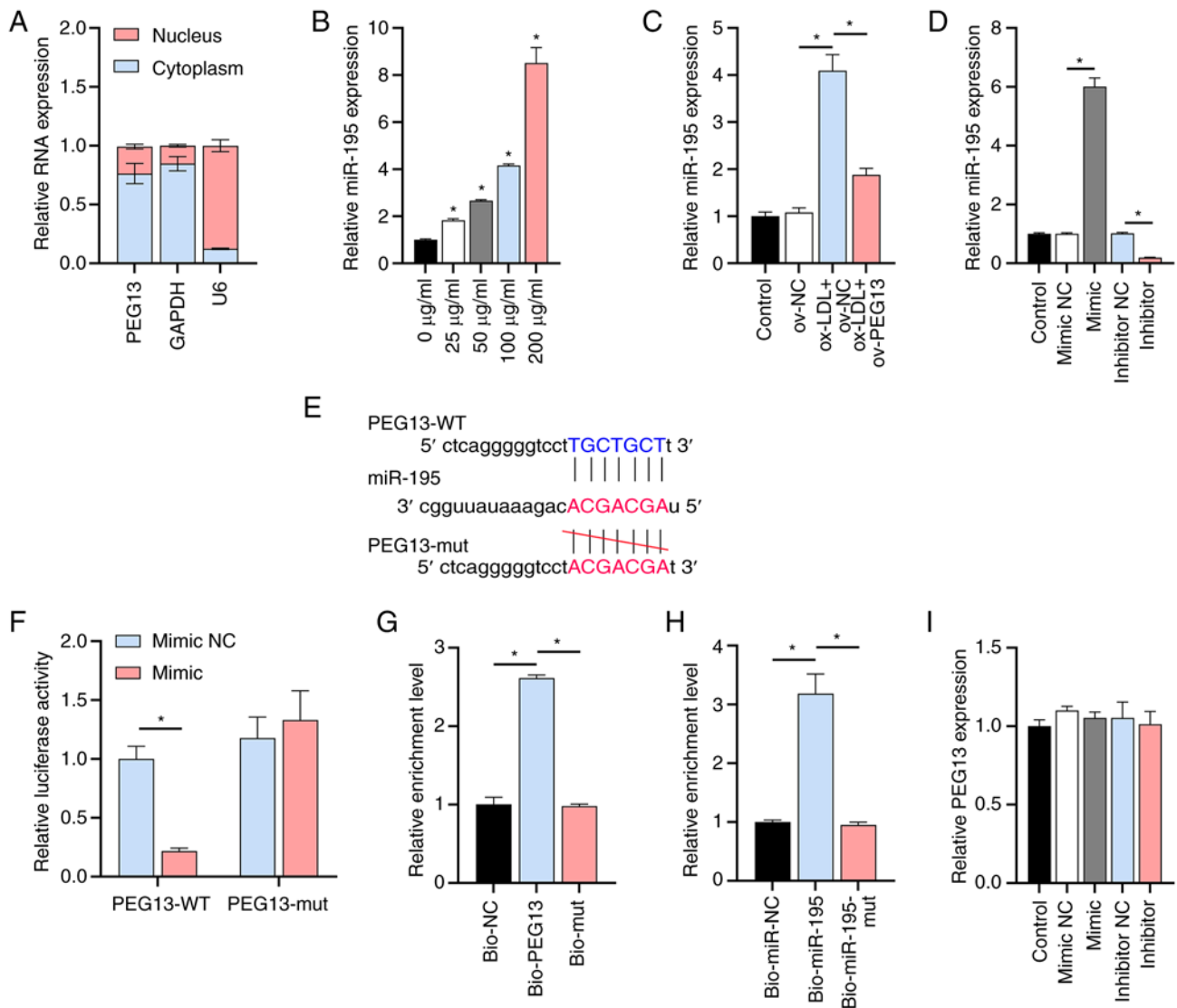
Figure 2. Interaction between lncRNA *PEG13* and miR-195 (A) Subcellular fractionation and RT-qPCR showing lncRNA *PEG13* localization. (B) Levels of miR-195 expression in the presence of various ox-LDL doses, as determined through RT-qPCR analysis (*P<0.05 vs. 0 μg/ml). (C) Level of miR-195 expression following *PEG13* overexpression, as determined through RT-qPCR analysis. (D) Validation of the synthesized miR-195 mimic/inhibitor. (E) TargetScan prediction of potential binding sites between miR-195 and IRS1. (F) Dual-luciferase reporter assay of the interaction between lncRNA *PEG13* and miR-195. (G and H) RNA pull-down assay demonstrating (G) miR-195 enrichment in Bio-*PEG13* and (H) *PEG13* enrichment in Bio-miR-195. (I) RT-qPCR analysis of the effect of the miR-195 mimic/inhibitor on *PEG13* expression. *P<0.05. lncRNA, long non-coding RNA; miR, microRNA; ox-LDL, oxidized low-density lipoprotein; RT-qPCR, reverse transcription-quantitative PCR; lncRNA, long non-coding RNA; WT, wild type; mut, mutant; ov, overexpression; NC, negative control.

revealed the overlap of three genes (Fig. 3A), among which *IRS1*, a potential miR-195 target, is a known activator of the PI3K/AKT pathway (25). The KEGG analysis indicated that the PI3K/AKT pathway was one of the major signaling pathways involved in atherosclerosis (Fig. 3B), further confirming the rationality of IRS1 involvement. The RT-qPCR assay results showed that ox-LDL decreased *IRS1* expression in a dose-dependent manner (Fig. 3C) and this downregulation was ameliorated by *PEG13* overexpression (Fig. 3D) and negatively regulated by miR-195 (Fig. 3E). Bioinformatics analysis revealed potential binding sites between *IRS1* and miR-195 (Fig. 3F) and the dual-luciferase reporter assay confirmed that the gene is indeed a direct target of this miRNA (Fig. 3G). The three small interfering RNAs (siRNAs) designed to target *IRS1* (si-*IRS1*) inhibited the expression of both the gene

(Fig. 3H) and its protein (Fig. 3I) in HUVECs, with siRNA-1 showing the highest inhibition rate in follow-up mechanistic experiments.

PEG13 overexpression enhanced PI3K/AKT signaling. Although the total protein levels of PI3K and AKT remained unchanged, *PEG13* overexpression, acting as an activator of the PI3K/AKT pathway, increased the phosphorylation of PI3K and AKT that had been reduced by ox-LDL (Fig. 4A). Next, the effect of the *PEG13*/miR-195/*IRS1* axis on PI3K/AKT expression was evaluated. The depletion of miR-195 via *PEG13* overexpression enhanced the activation of IRS1 protein level and PI3K/AKT signaling, but this effect was partially reversed by the suppression of *IRS1* expression (Fig. 4B). As expected, *PEG13* overexpression enhanced the
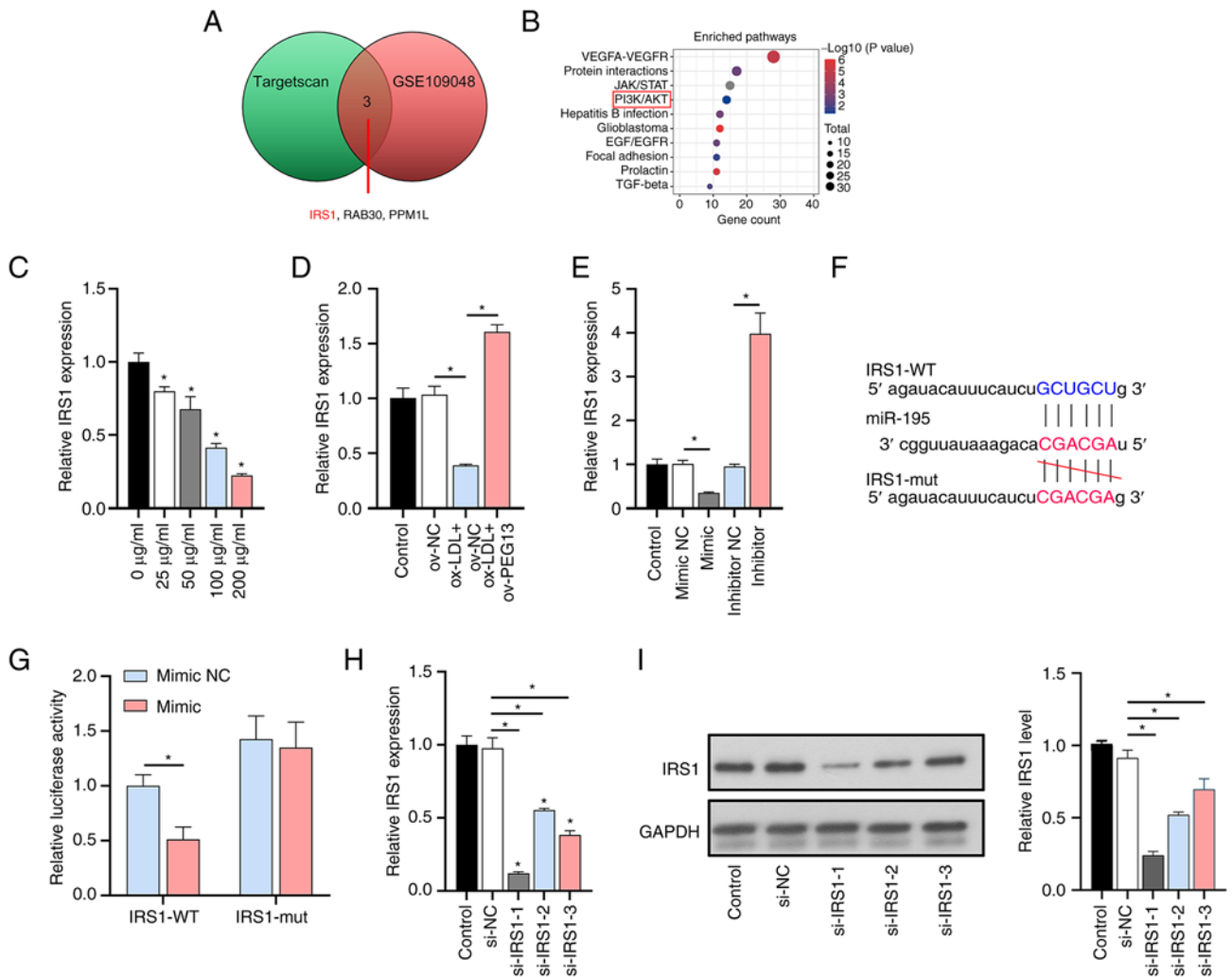
Figure 3. Involvement of IRS1 and the PI3K/AKT pathway in the lncRNA *PEG13*/miR-195 axis. (A) Venn diagram showing potential targets for lncRNA *PEG13*, determined from the joint analysis of TargetScan and GSE109048 datasets. (B) Bubble map showing genes involved in atherosclerosis-related pathways in the GSE109048 dataset. (C) Levels of *IRS1* expression in the presence of various doses of ox-LDL, as determined through RT-qPCR analysis (*P<0.05 vs. 0 μg/ml). (D) Levels of IRS1 expression following *PEG13* overexpression, as determined through RT-qPCR analysis. (E) Levels of *IRS1* expression after miR-195 mimic/inhibitor treatment, as determined through RT-qPCR analysis. (F) Potential binding sites between *IRS1* and miR-195, as determined through bioinformatics analysis. (G) Dual-luciferase reporter assay confirmation of *IRS1* as a direct target of miR-195. (H) Levels of *IRS1* expression in HUVECs transfected with siRNA, as determined through RT-qPCR analysis. (I) IRS1 protein levels in HUVECs transfected with siRNA, as determined through western blot analysis. *P<0.05. IRS1, insulin receptor substrate 1; lncRNA, long non-coding RNA; miR, microRNA; ox-LDL, oxidized low-density lipoprotein; RT-qPCR, reverse transcription-quantitative PCR; HUVECs, human umbilical vein endothelial cells; siRNA, small interfering RNA; WT, wild type; mut, mutant; ov, overexpression; NC, negative control.

positive effects of miR-195 depletion on cell viability (Fig. 4C) and angiogenesis (Fig. 4D), ameliorated senescence (Fig. 4E), reduced the IL-1β, IL-6 and IL-8 levels (Fig. 4F-H) and inhibited the ox-LDL-induced downregulation of MCP-1, VCAM-1 and ICAM-1 expression (Fig. 4I-K) and all these effects were partly reversed by si-*IRS1*.

PI3K/AKT signaling plays an essential role in cellular senescence. To further investigate the role of the PI3K/AKT pathway in ox-LDL-induced HUVEC senescence, LY294002 was used to inhibit PI3K signaling. As a result, the effects of *PEG13* overexpression in promoting MDM2 expression and inhibiting the senescence-associated proteins p53 and p21 were blocked in the presence of LY294002 (Fig. 5). This further indicates that the PI3K/AKT signaling pathway is essential for regulating HUVEC senescence, with *PEG13* acting as a key mediator in the process.

Discussion

Atherosclerosis can lead to cardiovascular diseases with high rates of morbidity and mortality, including ischemic stroke, coronary heart disease and myocardial infarction, thus posing a serious threat to human health (26,27). Understanding the role of lncRNAs in regulating gene expression is important for understanding the pathological mechanisms of atherosclerosis (28). In the present study, lncRNA *PEG13* was used as an entry point to analyze the effects of its downstream targets and signal transduction pathways on the pathogenesis and progression of atherosclerosis. One of the major findings was that ox-LDL reduced both the viability of HUVECs and their expression of lncRNA *PEG13* in a dose-dependent manner and these effects could be partially reversed through *PEG13* overexpression, thereby confirming for the first time
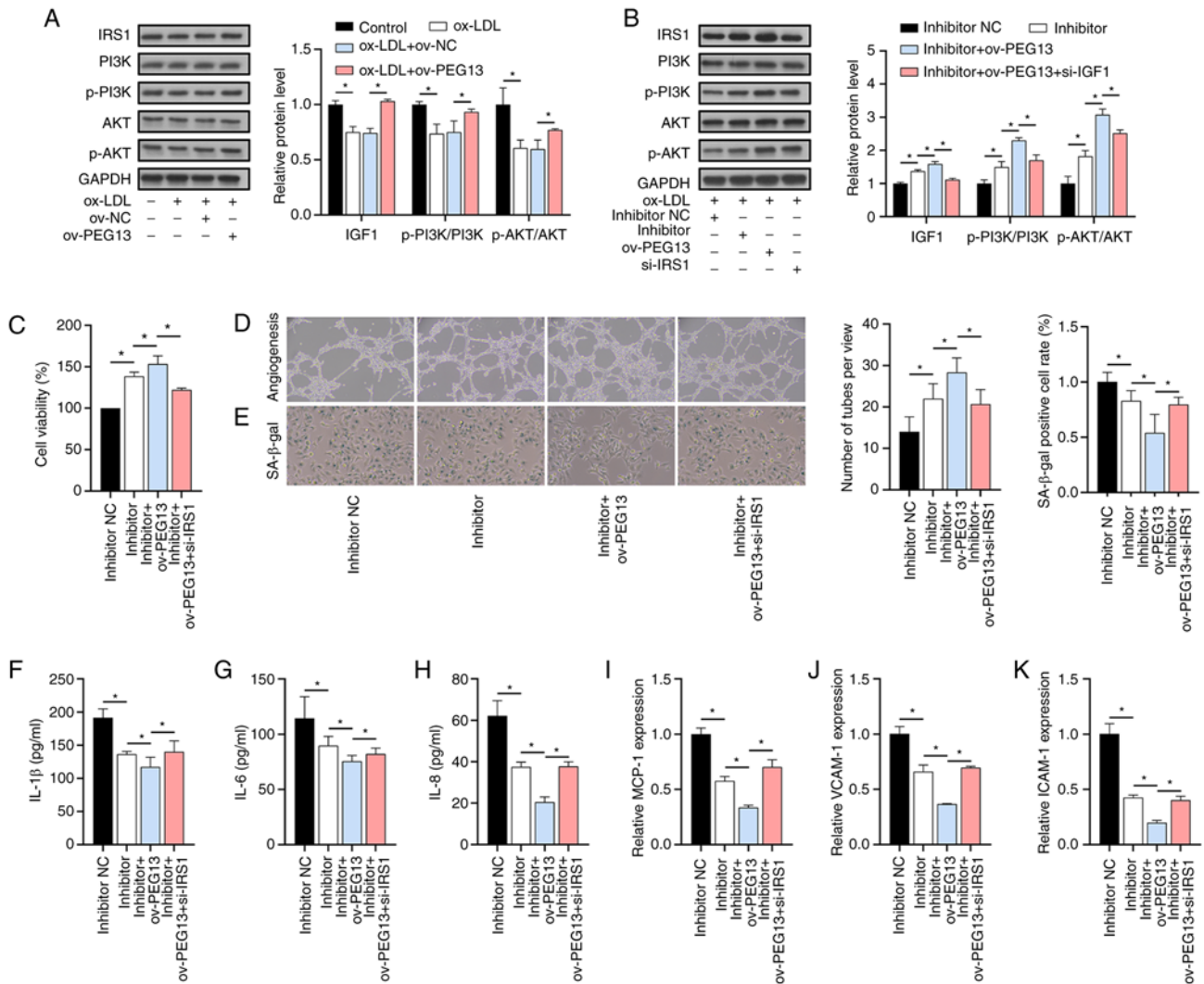
Figure 4. Activation of PI3K/AKT signaling by *PEG13* overexpression. (A) IRS1, p-PI3K, PI3K, AKT and p-AKT protein levels after *PEG13* overexpression, as determined through western blot analysis. (B) IRS1, p-PI3K, PI3K, AKT and p-AKT protein levels under *PEG13* overexpression, miR-195 depletion and IRS1 suppression conditions, as determined through western blotting. (C) Combined effects of *PEG13* overexpression and miR-195 depletion on cell viability, as determined with the MTT assay. (D) Angiogenesis changes due to *PEG13* overexpression and miR-195 depletion, as determined with the tube formation assay. Magnification, x200. (E) SA-β-gal staining showing the effects of *PEG13* overexpression and miR-195 depletion on senescence. Magnification, x200. (F) IL-1β, (G) IL-6 and (H) IL-8 protein levels following *PEG13* overexpression and miR-195 depletion, as measured with ELISA. Levels of (I) MCP-1, (J) VCAM-1 and (K) ICAM-1 expression following *PEG13* overexpression and miR-195 depletion, as determined through RT-qPCR analysis. *$P<0.05$. IRS1, insulin receptor substrate 1; p-, phosphorylated; miR, microRNA; MTT, 3-(4,5-dimethylthiazol-2-yl)-2,5-diphenyltetrazolium bromide; SA-β-gal, senescence-associated beta-galactosidase; MCP-1, monocyte chemoattractant protein-1; VCAM-1, vascular cell adhesion molecule-1; ICAM-1 and intercellular adhesion molecule-1; ov, overexpression; NC, negative control.
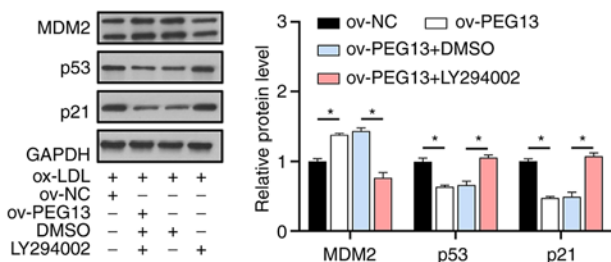
Figure 5. Role of the PI3K/AKT pathway in cellular senescence. Western blot analysis of MDM2, p53 and p21 protein levels after LY treatment, showing the impact of the PI3K/AKT pathway inhibition on *PEG13* overexpression-induced senescence reduction. *$P<0.05$. MDM2, MDM2 proto-oncogene; LY, LY294002; p53, tumor protein p53; p21, cyclin-dependent kinase inhibitor 1A (CDKN1A); ov, overexpression; NC, negative control; ox-LDL, oxidized low-density lipoprotein.

the involvement of lncRNA *PEG13* in the pathogenesis of atherosclerosis. Therefore, the present study also investigated the effect of lncRNA *PEG13* on HUVEC senescence and the underlying molecular mechanisms involved.

Consistent with previous research findings, the present results suggested that lncRNA *PEG13* serves as a critical modulator of endothelial cell senescence in response to ox-LDL exposure and its overexpression promotes HUVEC viability and ameliorates cellular senescence while downregulating the inflammatory cytokines IL-1β, IL-6 and IL-8 (29,30). Furthermore, the decrease in expression of the chemokines/adhesion molecules MCP-1, VCAM-1 and ICAM-1 implied decreased monocyte recruitment and reduced leukocyte adhesion and infiltration (31,32), which are beneficial for reducing inflammation and limiting atherosclerotic plaque
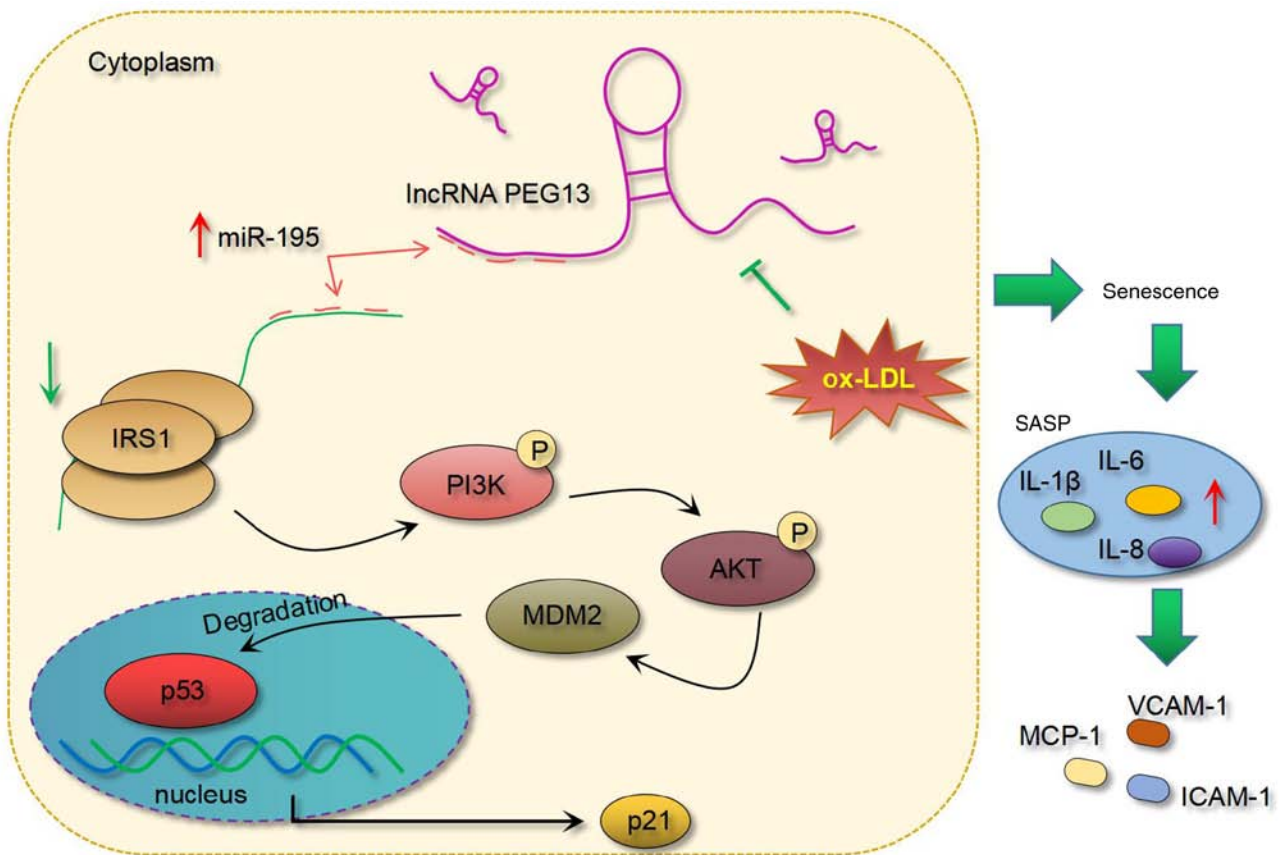
Figure 6. lncRNA *PEG13* activates the PI3K/AKT signaling pathway via the miR-195/IRS1 axis to promote the expression of MDM2 and inhibit that of age-related protein p53 and its downstream effector p21, leading to a decrease in both cells aging and the senescence-associated secretory phenotype. lncRNA, long non-coding RNA; miR, microRNA; ox-LDL, oxidized low-density lipoprotein; IRS1, insulin receptor substrate 1; MDM2, MDM2 proto-oncogene p53, tumor protein p53; p21, cyclin-dependent kinase inhibitor 1A (CDKN1A).

growth and instability, further supporting the anti-senescence and anti-inflammatory effects of lncRNA *PEG13* in HUVECs. Moreover, nucleocytoplasmic separation experiments revealed that lncRNA *PEG13* is predominantly expressed in the cytoplasm and may regulate cellular senescence through a competitive endogenous RNA mechanism (33).

Using LncBase predictions, dual-luciferase reporter assays and RNA pull-down assays, the present study first demonstrated the targeting of miR-195 by *PEG13*, a critical regulator of the pathogenesis of atherosclerosis (10). The IRS1/PI3K/AKT signaling pathway is involved in various biological processes, including cell survival, angiogenesis and senescence (34,35). In the present study, *IRS1* (an activator of the PI3K/AKT pathway) was found to be a target gene of miR-195, with ox-LDL promoting miR-195 expression and inhibiting *IRS1* expression in a dose-dependent manner. The suppression of *IRS1* expression counteracted the protective effects of *PEG13* and the miR-195 inhibitor and was associated with the deactivation of PI3K/AKT signaling. This is the first confirmation that *PEG13* regulates endothelial cell inflammation and senescence through the miR-195/IRS1 axis. Next, LY294002 (a PI3K inhibitor) was used to investigate the role of PI3K/AKT signaling in senescence. Previous studies have shown that this signaling pathway activates MDM2 and leads to the repression of p53 and p21, thereby promoting cell survival and reducing senescence (36,37). The expression of p53 and p21 increases in endothelial cells exposed

to various stressors, including ox-LDL, leading to endothelial dysfunction and plaque formation (38,39). In the present study, *PEG13*, which acted as an activator of PI3K/AKT signaling, upregulated the expression of MDM2 and attenuated the ox-LDL-induced increase in p53 and p21 levels, suggesting that the lncRNA *PEG13*/miR-195/IRS1/PI3K/AKT axis influences cellular senescence by modulating cell cycle regulators. The inhibition of PI3K signaling by LY294002 also inhibited downstream AKT signaling, resulting in increased expression of the senescence-related factor p53 and its downstream effector p21.

The present study had several limitations. First, within the context of atherosclerosis, HUVECs treated with ox-LDL serve as a mature model. The crux of our pursuit has been to delve deeply into the molecular mechanisms at play within this specific setting. As such, the present study did not branch out to encompass various cell types, such as smooth muscle cells, macrophages, or diverse immune cells. Second, the present study did not investigate co-culturing of HUVECs with other cellular forms. This restricts the holistic understanding of the role that lncRNA *PEG13* plays not only in atherosclerosis but also in pertinent *in vitro* systems. Third was the failure of the present study to conduct transcriptomic analysis, such as RNA-seq, on the ox-LDL treated cells. This would have elucidated any global transcriptional effects stemming from the ox-LDL treatment. Fourth, the present study did not venture into assessing the role of lncRNA *PEG13* within animal models, which is instrumental

in evaluating its potential as a therapeutic target. Finally, the authors have yet to extensively probe other potential targets and pathways influenced by this lncRNA. These gaps form the cornerstone of objectives for future research endeavors.

In conclusion, the present study demonstrated the protective role of lncRNA *PEG13* against ox-LDL-induced HUVEC dysfunction, an effect that involves its regulation of the IRS1/PI3K/AKT signaling pathway via miR-195 depletion and its subsequent influence on MDM2 and senescence-related factors p53 and p21 (Fig. 6). Future research based on these findings may contribute to the development of novel therapeutic strategies targeting lncRNA *PEG13* or its associated molecular pathways for the treatment and prevention of atherosclerosis.

Acknowledgements

Funding

Availability of data and materials

The datasets used and/or analyzed in the current study are available from the corresponding author upon reasonable request.

Authors' contributions

QH and HZ designed and developed the study methodology. QH, HZ and SY performed the experiments and collected and interpreted the data. QH and HZ drafted the manuscript. QH and HZ confirmed the authenticity of all raw data. All authors have read and approved the final version of the manuscript.

Ethics approval and consent to participate

Not applicable.

Patient consent for publication

Not applicable.

Competing interests

The authors declare that they have no competing interests.

References

1. Kong P, Cui ZY, Huang XF, Zhang DD, Guo RJ and Han M: Inflammation and atherosclerosis: Signaling pathways and therapeutic intervention. Signal Transduct Target Ther 7: 131: 2022.
2. Khatana C, Saini NK, Chakrabarti S, Saini V, Sharma A, Saini RV and Saini AK: Mechanistic insights into the oxidized low-density lipoprotein-induced atherosclerosis. Oxid Med Cell Longev 2020: 5245308, 2020.
3. Xiang Q, Tian F, Xu J, Du X, Zhang S and Liu L: New insight into dyslipidemia-induced cellular senescence in atherosclerosis. Biol Rev Camb Philos Soc 97: 1844-1867, 2022.
4. Vellasamy DM, Lee SJ, Goh KW, Goh BH, Tang YQ, Ming LC and Yap WH: Targeting immune senescence in atherosclerosis. Int J Mol Sci 23: 13059, 2022.
5. Honda S, Ikeda K, Urata R, Yamazaki E, Emoto N and Matoba S: Cellular senescence promotes endothelial activation through epigenetic alteration, and consequently accelerates atherosclerosis. Sci Rep 11: 14608, 2021.
6. Wu CM, Zheng L, Wang Q and Hu YW: The emerging role of cell senescence in atherosclerosis. Clin Chem Lab Med 59: 27-38, 2020.
7. Xu D, Dai R, Chi H, Ge W and Rong J: Long non-coding RNA MEG8 suppresses hypoxia-induced excessive proliferation, migration and inflammation of vascular smooth muscle cells by regulation of the miR-195-5p/RECK axis. Front Mol Biosci 8: 697273, 2021.
8. Wang Q, Deng F, Li J, Guo L and Li K: The long non-coding RNA SNHG1 attenuates chondrocyte apoptosis and inflammation via the miR-195/IKK-α axis. Cell Tissue Bank 24: 167-180, 2023.
9. Jin J, Wang C, Ouyang Y and Zhang D: Elevated miR-195-5p expression in deep vein thrombosis and mechanism of action in the regulation of vascular endothelial cell physiology. Exp Ther Med 18: 4617-4624, 2019.
10. Wang Y, Zhang CX, Ge SL and Gong WH: CTBP1-AS2 inhibits proliferation and induces autophagy in ox-LDL-stimulated vascular smooth muscle cells by regulating miR-195-5p/ATG14. Int J Mol Med 46: 839-848, 2020.
11. Gao H, Zhang Y, Xue H, Zhang Q, Zhang Y, Shen Y and Bing X: Long non-coding RNA Peg13 alleviates hypoxic-ischemic brain damage in neonatal mice via miR-20a-5p/XIAP axis. Neurochem Res 47: 656-666, 2022.
12. Jiang Y, Wang Y, Sun Y and Jiang H: Long non-coding RNA Peg13 attenuates the sevoflurane toxicity against neural stem cells by sponging microRNA-128-3p to preserve Sox13 expression. PLoS One 15: e0243644, 2020.
13. Wang N, Zhang X, Ma Z, Niu J, Ma S, Wenjie W and Chen J: Combination of tanshinone IIA and astragaloside IV attenuate atherosclerotic plaque vulnerability in ApoE(-/-) mice by activating PI3K/AKT signaling and suppressing TRL4/NF-κB signaling. Biomed Pharmacother 123: 109729, 2020.
14. Duan MX, Zhou H, Wu QQ, Liu C, Xiao Y, Deng W and Tang QZ: Andrographolide protects against HG-induced inflammation, apoptosis, migration, and impairment of angiogenesis via PI3K/AKT-eNOS signalling in HUVECs. Mediators Inflamm 2019: 6168340, 2019.
15. Cheng HW, Chen YF, Wong JM, Weng CW, Chen HY, Yu SL, Chen HW, Yuan A and Chen JJ: Cancer cells increase endothelial cell tube formation and survival by activating the PI3K/Akt signalling pathway. J Exp Clin Cancer Res 36: 27, 2017.
16. Chibaya L, Karim B, Zhang H and Jones SN: Mdm2 phosphorylation by Akt regulates the p53 response to oxidative stress to promote cell proliferation and tumorigenesis. Proc Natl Acad Sci USA 118: e2003193118, 2021.
17. Wu D and Prives C: Relevance of the p53-MDM2 axis to aging. Cell Death Differ 25: 169-179, 2018.
18. Sha JY, Li JH, Zhou YD, Yang JY, Liu W, Jiang S, Wang YP, Zhang R, Di P and Li W: The p53/p21/p16 and PI3K/Akt signaling pathways are involved in the ameliorative effects of maltol on D-galactose-induced liver and kidney aging and injury. Phytother Res 35: 4411-4424, 2021.
19. Cao YL, Liu DJ and Zhang HG: MiR-7 regulates the PI3K/AKT/VEGF pathway of retinal capillary endothelial cell and retinal pericytes in diabetic rat model through IRS-1 and inhibits cell proliferation. Eur Rev Med Pharmacol Sci 22: 4427-4430, 2018.
20. Li CY, Wang LX, Dong SS, Hong Y, Zhou XH, Zheng WW and Zheng C: Phlorizin exerts direct protective effects on palmitic acid (PA)-induced endothelial dysfunction by activating the PI3K/AKT/eNOS signaling pathway and increasing the levels of nitric oxide (NO). Med Sci Monit Basic Res 24: 1-9, 2018.
21. Wang Y, Zhang X, Zou C, Kung HF, Lin MC, Dress A, Wardle F, Jiang BH and Lai L: miR-195 inhibits tumor growth and angiogenesis through modulating IRS1 in breast cancer. Biomed Pharmacother 80: 95-101, 2016.
22. Miao M, Cao S, Tian Y, Liu D, Chen L, Chai Q, Wei M, Sun S, Wang L, Xin S, *et al*: Potential diagnostic biomarkers: 6 Cuproptosis- and ferroptosis-related genes linking immune infiltration in acute myocardial infarction. Genes Immun 24: 159-170, 2023.
23. Livak KJ and Schmittgen TD: Analysis of relative gene expression data using real-time quantitative PCR and the 2(-Delta Delta C(T)) method. Methods 25: 402-408, 2001.

24. Teng P, Liu Y, Zhang M and Ji W: Diagnostic and prognostic significance of serum miR-18a-5p in patients with atherosclerosis. Clin Appl Thromb Hemost 27: 10760296211050642, 2021.
25. Cui F and He X: IGF-1 ameliorates streptozotocin-induced pancreatic β cell dysfunction and apoptosis via activating IRS1/PI3K/Akt/FOXO1 pathway. Inflamm Res 71: 669-680, 2022.
26. Falk E: Pathogenesis of atherosclerosis. J Am Coll Cardiol 47 (8 Suppl): C7-C12, 2006.
27. Herrington W, Lacey B, Sherliker P, Armitage J and Lewington S: Epidemiology of atherosclerosis and the potential to reduce the global burden of atherothrombotic disease. Circ Res 118: 535-546, 2016.
28. Simion V, Zhou H, Haemmig S, Pierce JB, Mendes S, Tesmenitsky Y, Pérez-Cremades D, Lee JF, Chen AF, Ronda N, *et al*: A macrophage-specific lncRNA regulates apoptosis and atherosclerosis by tethering HuR in the nucleus. Nat Commun 11: 6135, 2020.
29. Jiang YH, Jiang LY, Wang YC, Ma DF and Li X: Quercetin attenuates atherosclerosis via modulating oxidized LDL-induced endothelial cellular senescence. Front Pharmacol 11: 512, 2020.
30. Cao H, Jia Q, Yan L, Chen C, Xing S and Shen D: Quercetin suppresses the progression of atherosclerosis by regulating MST1-mediated autophagy in ox-LDL-induced RAW264.7 macrophage foam cells. Int J Mol Sci 20: 6093, 2019.
31. Zhang Q, Liu J, Duan H, Li R, Peng W and Wu C: Activation of Nrf2/HO-1 signaling: An important molecular mechanism of herbal medicine in the treatment of atherosclerosis via the protection of vascular endothelial cells from oxidative stress. J Adv Res 34: 43-63, 2021.
32. Malekmohammad K, Sewell RDE and Rafieian-Kopaei M: Antioxidants and atherosclerosis: Mechanistic aspects. Biomolecules 9: 301, 2019.
33. Liu Y, Liu N and Liu Q: Constructing a ceRNA-immunoregulatory network associated with the development and prognosis of human atherosclerosis through weighted gene co-expression network analysis. Aging (Albany NY) 13: 3080-3100, 2021.
34. Kim W, Noh H, Lee Y, Jeon J, Shanmugavadivu A, McPhie DL, Kim KS, Cohen BM, Seo H and Sonntag KC: MiR-126 regulates growth factor activities and vulnerability to toxic insult in neurons. Mol Neurobiol 53: 95-108, 2016.
35. Perluigi M, Pupo G, Tramutola A, Cini C, Coccia R, Barone E, Head E, Butterfield DA and Di Domenico F: Neuropathological role of PI3K/Akt/mTOR axis in down syndrome brain. Biochim Biophys Acta 1842: 1144-1153, 2014.
36. Huang L, Ye Q, Lan C, Wang X and Zhu Y: AZD6738 Inhibits fibrotic response of conjunctival fibroblasts by regulating checkpoint kinase 1/P53 and PI3K/AKT pathways. Front Pharmacol 13: 990401, 2022.
37. Safi A, Heidarian E and Ahmadi R: Quercetin synergistically enhances the anticancer efficacy of docetaxel through induction of apoptosis and modulation of PI3K/AKT, MAPK/ERK, and JAK/STAT3 signaling pathways in MDA-MB-231 breast cancer cell line. Int J Mol Cell Med 10: 11-22, 2021.
38. Lyu TJ, Zhang ZX, Chen J and Liu ZJ: Ginsenoside Rg1 ameliorates apoptosis, senescence and oxidative stress in ox-LDL-induced vascular endothelial cells via the AMPK/SIRT3/p53 signaling pathway. Exp Ther Med 24: 545, 2022.
39. Liu Y, Jia L, Min D, Xu Y, Zhu J and Sun Z: Baicalin inhibits proliferation and promotes apoptosis of vascular smooth muscle cells by regulating the MEG3/p53 pathway following treatment with ox-LDL. Int J Mol Med 43: 901-913, 2019.